Double Pendulum

J. Robinson[a], J. Blumoff, M. Clark, S. Rah

[a] *Georgia Institute of Technology*
School of Aerospace Engineering
Aerospace Systems Design Laboratory
Atlanta, GA 30332-0150 U.S.A.

Abstract

This paper describes physical experimentation and numerical simulation with a double pendulum. Initial emphasis was on experimenting with a double pendulum with an oscillating suspension point. While experimentation with that system was performed, difficulties with data acquisition meant that only the non-driven case received detailed attention. The double pendulum was tracked with a high speed camera. Image processing programs transformed the video data into useable angle measurements. The time until the first flip of the second arm was measured for many different combinations of initial angles. A more thorough exploration of this same metric was performed using numerical simulation, first with WorkingModel2D, then with MATLAB. Experimental and numerical results agreed qualitatively, although the resolution of the numerical work was much higher.

Keywords: double pendulum, chaos, image processing

1. Introduction and Background

The double pendulum is a chaotic system as is expected [1, 2], since it is nonlinear and has a phase space of more than two dimensions. As such small differences in initial conditions grow at $O(e^t)$ [1]. Due to its simplicity and rich dynamical behavior, this system is widely used in introducing the concept of chaos [2]. Many introductory experiments use a driven double pendulum, as this permits longer periods of data gathering before damping of the system [2]. This driving typically takes the form of a motor driving the first joint of the pendulum in an oscillatory manner. An example of this is [3] which examined bifurcations leading to low-dimensional chaos using an apparatus of this nature.

The dynamic equations of an ideal double pendulum, as described in Figure 1., can be found via the Euler-Lagrange equations of motion. First the potential energy and kinetic energy of the system are determined [1]:

$$V = \ell_1(1-\cos\theta_1)m_1 g + [\ell_1(1-\cos\theta_1) + \ell_2(1-\cos\theta_2)]m_2 g$$

Email address: jrobinson@asdl.gatech.edu (J. Robinson)

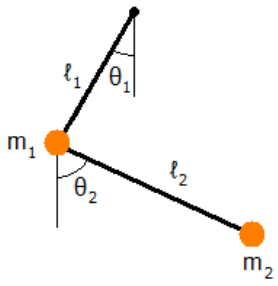

Figure 1: Ideal double pendulum

$$T = \frac{1}{2}(m_1+m_2)\ell_1^2\dot{\theta}_1^2 + \frac{1}{2}m_2\ell_2^2\dot{\theta}_2^2 + m_2\ell_1^2\ell_2^2\dot{\theta}_1^2\dot{\theta}_2^2\cos(\theta_1-\theta_2) \quad (1)$$

Now, applying the Euler-Lagrange equations we get [1]:

$$\begin{aligned} \cos(\theta_1-\theta_2)\ddot{\theta}_1 + \frac{\ell_2}{\ell_1}\ddot{\theta}_2 &= \dot{\theta}_1^2\sin(\theta_1-\theta_2) - \frac{g}{\ell_1}\sin\theta_2 \\ \cos(\theta_1-\theta_2)\ddot{\theta}_2 + \frac{(1+\frac{m_1}{m_2})\ell_2}{\ell_1}\ddot{\theta}_1 &= -\dot{\theta}_2^2\sin(\theta_1-\theta_2) - \frac{g(1+\frac{m_1}{m_2})}{\ell_1}\sin\theta_1 \quad (2) \end{aligned}$$

After separating, this yields [1]:

$$\begin{aligned} \ddot{\theta}_1 &= \frac{g(\sin\theta_2\cos(\theta_1-\theta_2) - (1+\frac{m_1}{m_2})\sin\theta_1) - (\ell_2^2\dot{\theta}_2^2 + \ell_1^2\dot{\theta}_1^2\cos(\theta_1-\theta_2))\sin(\theta_1-\theta_2)}{\ell_1((1+\frac{m_1}{m_2}) - \cos^2(\theta_1-\theta_2))} \\ \ddot{\theta}_1 &= \frac{g(1+\frac{m_1}{m_2})(\sin\theta_1\cos(\theta_1-\theta_2) - \sin\theta_2) - ((1+\frac{m_1}{m_2}\ell_1^2\dot{\theta}_1^2 + \ell_2^2\dot{\theta}_2^2\cos(\theta_1-\theta_2))\sin(\theta_1-\theta_2)}{\ell_2((1+\frac{m_1}{m_2}) - \cos^2(\theta_1-\theta_2))} \quad (3) \end{aligned}$$

Both of these equations are second order nonlinear differential equations, indicating a 4-D phase space.

By adding oscillation of the suspension point, the phase space of the system is increased from 4-D to 6-D. Linear oscillation of single pendulums has been explored in the past as a means of stabilizing the fixed point at $\theta = \pi$. Only one study is known to have explored this technique for the double pendulum [4]. The conclusion was that the fixed point $\theta_1^* = \pi$, $\theta_2^* = \pi$ is stable for the case $\Omega^2 > \frac{g}{a^2}[l_1+l_2+\sqrt{l_1^2+l_2^2+2l_1l_2\frac{m_2-m_1}{m_1+m_2}}]$, where Ω is the frequency of suspension point oscillation, and m_1 and m_2 are the masses of the first and second arm (not point masses in this case.) [4]

2. Data Acquisition

The physical apparatus is shown in Figure 2. It consists of a double pendulum suspended by an axle supported by two metal frames. The frames are

connected to a shaker which can oscillate the entire apparatus at different frequencies and amplitudes. The apparatus was not capable of oscillating at the frequencies necessary to test inverted stability.

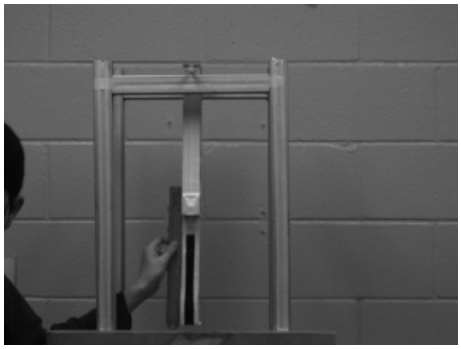

Figure 2: The apparatus

The initial plan for tracking the pendulum was to measure the acceleration of the second arm using an Analog Devices ADXL321 accelerometer. This method was abandoned for two reasons. First, it was very difficult to extract actual angular measurements from the radial and tangential accelerations provided by the accelerometer. Second, and perhaps the more insurrmountable of the two, the data resolution provided by the accelerometer was insufficient to yield clear data, even after filtering.

The next method attempted was to track points (LEDs) on the pendulum using a high-speed camera. This method showed some promise, but was also discarded. The problem with this approach was that small search boxes in the point tracking program lost the LEDs when they crossed behind an obstructing support. Search boxes which were large enough to relocate the LEDs proved unstable, with too much of the search box going out of the frame of view.

The data acquisition method that was decided on was line-tracking using a high-speed camera. A piece of black tape was placed on the second arm of the pendulum for tracking. By opening the aperture of the camera to its maximum, the image got "washed out" showing nothing but the black tape. Theoretically, by tracking the slope of the second arm and making a few a few measurements from reference images, one can extrapolate the angles of both arms at each time step. This processing was not done in real time however. Instead the video images were captured and saved for later processing.

3. Data Processing

Following the video capture of the pendulum, substantial image processing of the raw data is required to extract meaningful results. The raw data is in the form of 320 x 240 pixel 8-bit grayscale .bmp files (see Figure 3.) The video

was captured at a rate of 100 frames/second. First the processing for the non-driven double pendulum cases will be presented, followed by a discussion of adjustments necessary for tracking the driven double pendulum.

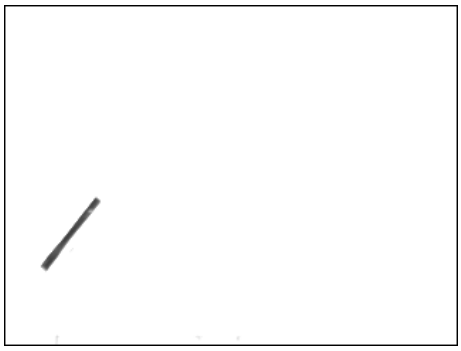

Figure 3: Raw video frame

3.1. Non-driven case

Each image frame is converted into a binary image using a threshold of 150 out of 255 for an 8-bit image. The image is then morphologically opened, that is eroded and then dilated, to remove small imperfections in the binary image. Following opening, the "thin" morph is applied to the image. This morph removes all boundary (outside edge) pixels from the image unless it would break a region into two or more non-contiguous regions. The result of this morph is the "skeleton" of the image. After morphing to this skeleton structure, the endpoint morph is applied. This morph finds the endpoints of the skeleton, that is pixels only connected to one other pixel.

Figure 4: Frame converted to binary image, then thinned

The slope of the second pendulum arm is determined using the endpoints, by performing a polynomial fit of degree one, that is linear regression. Using this small amount of points yields much better results than regression all points in

the binary image. A rough centroid of the second arm is found by determining the average coordinate of all of the 1 pixels in the skeleton image.

3.1.1. Time to flip

Using the slope and the centroid, a flip of the second arm can be detected as a change in the sign of the slope, m, when the centroid is within the circle traced out by the tip of the first arm. This change in sign is a necessary but insufficient condition for a flip. In addition, a check is made to make sure the slope crossed from $-\infty$ to ∞ or vice-versa, and didn't just cross 0. This is ensured by confirming that both $|m|_{i-1}$ and $|m|_i > 1$. In summary the conditions for a flip at timestep i are:

$$\begin{aligned} sgn(m_{i-1}) &\neq sgn(m_{i-1}) \\ |m|_{i-1} &> 1 \\ |m|_i &> 1 \\ (x_{sus} - x_{cent})^2 + (y_{sus} - y_{cent})^2 &< \ell_1^2 \end{aligned} \tag{4}$$

In equation (4), x_{sus} and y_{sus} refer to the x and y coordinates of the suspension point of the pendulum, while x_{cent} and y_{cent} refer to the x and y coordinates of the "rough" centroid of the second arm. The coordinates of the suspension point were found from an image taken prior to video capture, during which a piece of black tape was placed over that point. Additionally, $/ell_1$ is the length of the first arm of the pendulum (in pixels). This was likewise obtained from a reference image frame, this time captured with the aperture at a normal setting so as not to wash out features.

Finding the first i to satisfy these equations is not adequate to determine time to flip, however. The video capture often begins with several seconds of the arms being held at stationary initial conditions (within the limits of the human operator to hold said arms steady). It may be possible to write a program to intelligently determine the point at which the pendulum is released, but in this analysis, this point is simply identified by human examination of slope data. The timestep at which the slope begins to change significantly is considered the release time step.

3.1.2. Angle tracking

The previous section detailed the manner in which time to flip could be extrapolated from the video data. This time to flip is intended to be correlated to different initial conditions. Slope data alone is not sufficient to determine θ_2, the angle of the second arm. A given slope can correspond to two different angles in the range $-\pi < \theta_2 < \pi$. A reasonable method to determine the correct angle is as follows:

1. Find the points of intersection between the regression line and the circle, $(x_{sus} - x)^2 + (y_{sus} - y)^2 = \ell_1^2$. One of these points is the location of the joint between the first and second arms of the pendulum.
2. If $(x_{sus} - x_{cent})^2 + (y_{sus} - y_{cent})^2 > \ell_1^2$, go to 3. Otherwise, go to 4.

3. Of the two points identified in 1., the one which is closer to the centroid is the joint, whose coordinates will be referred to as x_{joint} and y_{joint}. The angles are found by $\theta_{1_i} = arctan2((y_{sus} - y_{joint}, x_{sus} - x_{joint})$ and $\theta_{2_i} = arctan2((y_{sus} - y_{cent}, x_{sus} - x_{cent})$. In these equations, arctan2 is the four-quadrant arctangent function. Done.
4. In this case, the point closer to the centroid need not be the joint. A more accurate means to determine angle is to simply choose the possible θ_{2_i} closer to $\theta_{2_{i-1}}$, the angle from the previous time step. The angle is found by $\theta_{2_i} = \arctan(m_i)$. The alternate possible angle is $\theta_{2_{i,alt}} = \theta_{2_i} + \pi$, with the caveat that if $\theta_{2_{i,alt}} > \pi$, then $\theta_{2_{i,alt}} - 2\pi \rightarrow \theta_{2_{i,alt}}$ (to keep angles within $-\pi < \theta < \pi$.) The only exception to this is when the second arm flips. In this case, specified in equation (4), the higher θ_{2_i} is chosen if $\theta_{2_{i-1}} < 0$, otherwise the lower θ_{2_i} is selected. From the location of the centroid and to removal of the angle ambiguity, it is now possible to determin the correct location of the joint. If $\theta_{2_i} > 0$ then the correct joint is the joint for which $x_{cent} - x_{joint} < 0$, otherwise, the correct joint is the one for which $x_{cent} - x_{joint} > 0$. Once the joint is identified, θ_1 can be identified as $\theta_{1_i} = arctan2((y_{sus} - y_{joint}, x_{sus} - x_{joint})$. Done.

There are some issues with this method, and occasionally, the wrong joint point is still selected, but it is usually corrected within a few time steps.

3.2. Driven case

The procedure for the driven cases is basically the same. The area around the suspension point is excluded from the binary image, even if the values surpass the threshold. x_{sus} and y_{sus} are determined by finding the centroid of the region (from the actual grayscale image to improve resolution). Apart from this, the procedure is identical.

4. Analysis of experimental data

Data from 47 runs of the pendulum, from different initial conditions are presented in Table 1.

An example of typical results from one run is shown in Figure 5. Note the flaws in the θ_1 case, especially during rapid flipping.

While in depth analysis of the driven cases was not achieved, due to the time spent working to obtain good data for the undriven case, runs of the driven cases were successfully processed. Results from one run are shown in Figure 6.

5. Numerical Modeling

The main effort in numerical modeling was an extension of the time to flip measurements undertaken in the physical experiment. The objective was to map starting angles, θ_1 and θ_2 to time to flip for a large sampling of initial conditions, with the objective of generating a fractal image representing this

Table 1: Time to flip

θ_1	θ_2	t_{flip}	θ_1	θ_2	t_{flip}
-2.144	0.369	0.76	-1.239	-0.2171	0.68
-1.953	0.1938	0.58	-1.233	-0.396	3.17
-1.747	-1.452	4.12	-1.194	-0.1033	0.58
-1.711	-2.155	1.34	-1.193	-0.5809	n/a
-1.704	-2.593	1.2	-1.183	-1.418	n/a
-1.674	-0.7623	2.64	-1.165	-1.416	n/a
-1.658	-2.301	1.36	-1.159	-0.5001	n/a
-1.527	-0.3931	0.63	-1.157	-0.1481	1.29
-1.484	-0.4667	0.58	-1.154	-0.1529	1.41
-1.48	-2.661	1.27	-1.094	-0.1134	0.59
-1.467	-0.4623	0.63	-1.086	-1.293	n/a
-1.446	-2.481	3.98	-1.058	0.2018	0.58
-1.443	-1.443	n/a	-1.05	-0.3393	n/a
-1.432	-2.318	n/a	-0.9935	-1.599	n/a
-1.414	-0.4025	1.41	-0.9864	0.04563	n/a
-1.408	-0.5585	n/a	-0.966	-1.492	n/a
-1.391	-2.5463	1.89	-0.9638	-2.369	n/a
-1.377	-0.4676	1.24	-0.8028	0.1243	n/a
-1.375	-0.6127	3.88	-0.7889	0.5277	n/a
-1.353	-0.6593	n/a	-0.7729	0.09	n/a
-1.338	-2.13	n/a	-0.6174	-2.833	n/a
-1.308	0.3539	0.75	-0.5765	-0.661	n/a
-1.302	2.518	0.9	-0.5602	-1.572	n/a
-1.267	-2.468	1.89			

mapping. In the interest of obtaining as high a resolution as possible, it was useful to determine sets of initial conditions which did not need to be tested. Some initial conditions could be excluded as they lacked the requisite potential energy for a flip. The energy in excess of the ground state needed to reach a flipping configuration is given by

$$E_{Minimumtoflip} = [(m_1 b_1) + m_2(l - b_2)]g \tag{5}$$

Since the initial angular velocities are zero, the greatest amount of energy in the system is the initial sum of the gravitational potential energies of the two arms. If this is less than the minimum energy to flip, the system can not flip with those starting conditions. In this manner many cases can be culled from the simulation. Additionally, it shoud be noted that the dynamics of the system are symmetric with regards to the initial θ_1. A positive or negative starting θ_1 yields the same trajectories, merely flipped across the y-axis. For this reason, it is only necessary to simulate positive θ_1s.

The first tool used to numerically simulate the double pendulum dynamics

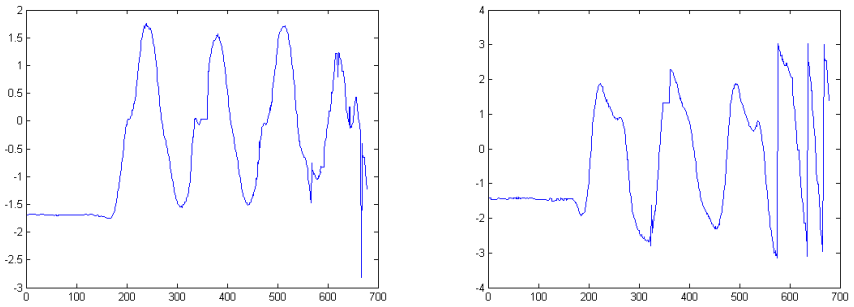

Figure 5: θ_1 and θ_2 vs. time

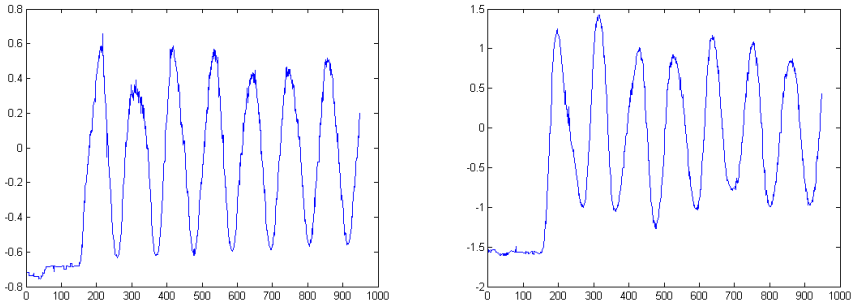

Figure 6: θ_1 and θ_2 vs. time (driven case)

was WorkingModel2D. A replica of the physical apparatus was created in the program. Using WorkingModel's BASIC-based programming language, WMBasic it was possible to run batches of initial conditions waiting for the system to flip or a maximum time step to be reached. This method had some notable limitations. Attempts to make the integration run faster than real-time were unsuccesful. As a result, exploring both $\phi_{1,init}$ and $\phi_{2,init}$ from 0 to 180 degrees in 1 degree steps took approximately 12 hours of computer time. Additionally, WMBasic will only allow access to the data in larger steps intervals. This results in poor temporal resolution for time to flip measurements.

Despite the limitations of this model, a fractal pattern was generated. As shown in Figure 7, both a large area graph and a zoomed in region were explored. In both cases, resolution for both initial conditions and time to flip were poor, suggesting a better method of simulation might be advisable.

Instead of using specialized dynamic simulation software, the equations of motion for the double pendulum were simply numerically integrated in MATLAB. This simulation was considerably faster than that performed in WorkingModel2D. The full $-\pi$ to π range was explored for both $\phi_{1,init}$ and $\phi_{2,init}$ in this simulation, with 370 points in each dimension. The image generated is shown

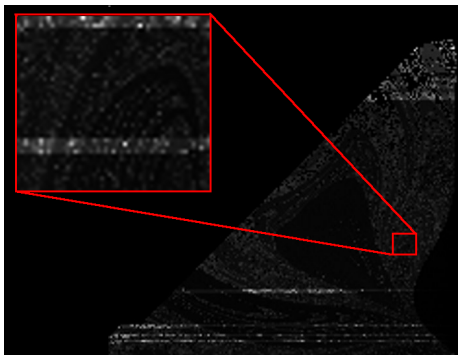

Figure 7: Fractal image generated from working model simulation

in Figure 8.

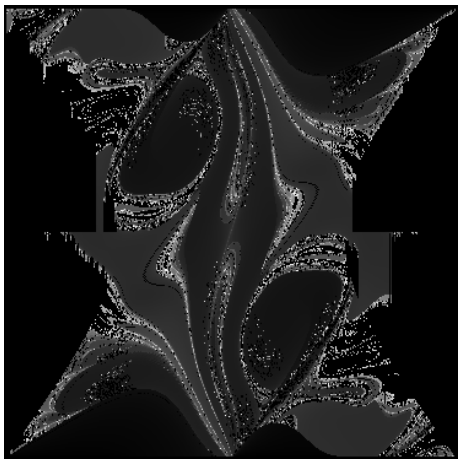

Figure 8: Fractal image generated from MATLAB numerical integration

It is worth noting that the horizontal axis in this image (which represents values of θ_1) actually ranges from 0 to $-\pi$, then from π to 0. This setup of the axis most clearly represents the pattern generated.

Now that both physical experimentation and numerical simulation have explored the time to flip, the results from the two can be compared. Figure 9. shows the fractal with the experimental results overlayed. Red squares indicate cases that did not flip, while green squares indicate flips (with intensity corresponding to time to flip.) A reasonable level of correlation is evident between the two.

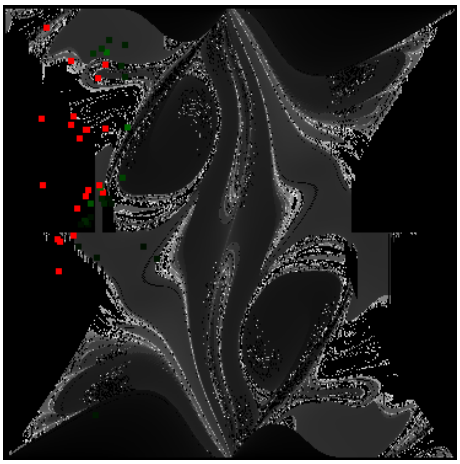

Figure 9: Fractal image with experimental results overlayed

6. Conclusion

The rich dynamical behavior of the double pendulum is a daunting system to explore. While this project began with the intention of exploring the ful 6-D phase space of a double pendulum with an oscillating suspension point, even the non-oscillating pendulum proved a challenging system to analyze. The greatest limitation on this research was the amount of effort required to acquire data in the physical experimentation. While the system for achieving this objective presented in this paper is not fully developed and has limitations, it shows promise for yielding high-quality data. Some of the difficulties could be assuaged by constructing an aparatus with a cantilevered suspension point, removing obstructing beams when visually tracking the pendulum.

Despite difficulties and deviation from the initial objectives, this project has provided valuable insight into the chaotic behavior of the double pendulum system. Experimental results were displayed which corroborated information provided by a fractal generated by numerical integration of a more ideal system. It is clear that physical experimentation is a valid and valuable means to explore the system, providing a useful comparison to theoretical and numerical research.

[1] Troy Shinbrot, Celso Grebogi, Jack Wisdom, and James A. Yorke, "Chaos in a double pendulum," Am. J. Phys., vol. 60, no. 6, pp. 491-499, June 1992.

[2] R. B. Levien and S. M. Tan, "Double pendulum: An experiment in chaos," Am. J. Phys., vol. 61, no. 11, pp. 1038-1044, November 1993.

[3] Peter Jäckel and Tom Mullin, "A numerical and experimental study of codimension-2 points in a parametrically excited double pendulum," Proc. R. Soc. Lond. A, vol. 454, pp. 3257-3274, 1998.

[4] O. V. Kholostova, "On the motions of a double pendulum with vibrating suspension point," Mechanics of Solids, vol. 44, no. 2, pp. 184-197, April 2009.